JOURNAL OF PROPULSION AND POWER
Vol. 12, No. 3, May–June 1996

Theory of Unsteady Combustion of Solids: Investigation of Quasisteady Assumption

Maria A. Zebrowski* and M. Quinn Brewster†
University of Illinois at Urbana–Champaign, Urbana, Illinois 61801

A numerical model was developed to investigate the applicability of activation energy asymptotics (AEA) in unsteady combustion of solids, and specifically, the quasisteady condensed phase (surface) reaction assumption. It was found that while condensed phase global decomposition activation energies are typically large enough for accurate prediction of steady burning rate and surface temperature by AEA, the criterion for comparable accuracy in predicting unsteady burning rate (e.g., linear response function) is more stringent. For realistic material properties the error in the linear response because of the quasisteady condensed phase reaction assumption is significant, both in magnitude and phase. The results also show that at moderate pressures (10–100 atm), condensed phase reaction zone unsteadiness should be considered before, or at least in conjunction with, gas phase unsteadiness. Nonlinear combustion response was also investigated. The primary effect of nonlinearity was to convert low-frequency response (particularly that near the peak) to higher frequencies. Validation of numerical results was accomplished by comparing the linear surface reaction response with the predictions of analysis.

Nomenclature

A = pre-exponential factor in zeroth order, condensed phase global reaction rate expression, $A\rho_c \exp(-E_c/RT)$
C = specific heat of condensed phase
E_c = effective activation energy of condensed phase decomposition reaction
E_s = $E_c/2$
f = frequency, Hz
f, g = general functions in Eqs. (13) and (14)
f_r = fraction of q absorbed below surface reaction zone
f_s = surface temperature gradient, $(\partial T/\partial x)_s$
J = dimensionless mean radiant heat flux, $\bar{q}/[\bar{m}C(\overline{T}_s - T_0)]$
K_a = radiation absorption coefficient of condensed phase
k = $(\overline{T}_s - T_0)(\partial\ \ell n\ \overline{r}_b/\partial T_0)_{p,q}$
k_c = thermal conductivity, $\alpha_c\rho_c C$
m = mass burning rate, $\rho_c r_b$
m' = $\Delta m e^{i(\omega t+\phi)}$
n_q = $(\partial\ \ell n\ \overline{r}_b/\partial\ \ell n\ \bar{q})_{T_s,p}$, $(=\delta_q/r)$
p = pressure
Q_c = chemical heat release by condensed phase reaction, positive exothermic
QSC = quasisteady condensed phase reaction zone
QSHOD = quasisteady gas phase and condensed phase reaction zone, homogeneous propellant, one-dimensional heat feedback
QSG = quasisteady gas phase
q = absorbed radiant heat flux
q' = $\Delta q e^{i\omega t}$
q_c = conductive heat flux to surface from gas phase
R_q = radiation-driven linear frequency response function, $(m'/\bar{m})/(q'/\bar{q})$ at constant p
r = $(\partial\overline{T}_s/\partial T_0)_{p,q}$
r_b = burning rate
T_0 = initial temperature
T_s = surface temperature
x = coordinate normal to surface, positive into gas phase
x_c = inert condensed phase heated layer (convective–diffusive zone) thickness, $\alpha_c/\overline{r}_b$
x_R = condensed phase reactive–diffusive zone thickness, $2R\overline{T}_s x_c/E_c$
x_r = condensed phase radiation absorption zone length scale, $1/K_a$
Y = mass fraction of unreacted solid
α_c = condensed phase thermal diffusivity
β_r = optical thickness (absorption only) of inert, conduction zone, $K_a x_c$
Δ = amplitude of fluctuating quantity
δ_q = Jacobian parameter, $\nu_q r - \mu_q k$
θ = dimensionless temperature, $(T - T_0)/(\overline{T}_s - T_0)$
λ = $\frac{1}{2} + (\frac{1}{2})(1 + 4i\Omega)^{1/2}$
μ_q = $[1/(\overline{T}_s - T_0)](\partial\overline{T}_s/\partial\ \ell n\ \bar{q})_{T_0,p}$
ν_q = $(\partial\ \ell n\ \overline{r}_b/\partial\ \ell n\ \bar{q})_{T_0,p}$
ξ = x/x_c
ρ_c = condensed phase density
ϕ = response function phase angle
Ω = dimensionless frequency, $\omega\alpha_c/\overline{r}_b^2$, or reaction rate term
ω = $2\pi f$, angular frequency, rad/s

Subscripts
c = condensed phase or convective–diffusive
R = reaction
r = radiation
s = surface

Superscripts
$\bar{}$ = steady condition or mean value
$'$ = complex fluctuating quantity
$+/-$ = gas or condensed phase side of surface

Received April 5, 1995; revision received Jan. 2, 1996; accepted for publication Jan. 11, 1996.

*Graduate Research Assistant, Department of Mechanical and Industrial Engineering.
†Professor of Mechanical Engineering. Associate Fellow AIAA.

Introduction

THE classical theory of unsteady combustion of homogeneous solid propellants and energetic materials is based

on the assumption of a quasisteady (QS) reaction zone in the condensed phase (QSC) and a quasisteady gas phase (QSG). In the U.S. this theory (also called QSHOD for quasisteady, homogeneous, one dimensional) was developed in the context of the flame modeling (FM) approach, whereas in the former Soviet Union the phenomenological Zeldovich–Novozhilov (ZN) approach was used. In both approaches the condensed phase reaction description commonly employed, which tacitly includes the QSC assumption, has been that of a surface reaction, which condition can be formally justified by a high effective decomposition energy of activation. Usually either a simple ($n_s = 0$) or modified ($n_s \neq 0$) Arrhenius surface pyrolysis relation, $r_b = A_s p_{n_s} \exp(-E_s/RT_s)$, has been used.

For all of the effort that has been expended in quasisteady modeling (either by FM or ZN), the degree of quantitative success in predicting experimental results has been limited. There are probably several reasons for this,[1] including uncertainty regarding the validity of the QS assumptions. While several studies have relaxed the QSG assumption,[2,3] little work has been reported in investigating the validity of the QSC (surface) reaction assumption. This is somewhat ironic since breakdown of the QSC assumption might be expected to occur before (at lower frequencies than) breakdown of the QSG assumption,[4] depending on decomposition activation energy and pressure (high pressures and high activation energies are conducive to gas phase unsteadiness becoming important at lower frequencies than decomposition zone unsteadiness).

Perhaps the first study to recognize the possible importance of a distributed condensed phase reaction zone was that of Culick.[5] That study presented many parametric calculations showing how condensed phase distributed reaction might affect the response function. The analysis assumed spatially constant heat release over a thin layer near the surface; the species equation was not solved. This approach avoids the nonlinear problem introduced by temperature-dependent decomposition kinetics, but it also loses the ability to solve for the burning rate eigenvalue. Instead, a burning rate expression (such as a modified Arrhenius pyrolysis law) must be introduced ad hoc. This approach also requires that additional assumptions be made for the heat release sensitivity parameters and the decomposition reaction zone thickness. These problems can be avoided by formally including the species equation and an appropriate reaction rate expression, and solving the eigenvalue problem for burning rate using asymptotic methods (large activation energy), as pointed out in a later paper (for gas phase reaction) by Williams.[6] Subsequently, Lengelle et al.[7] developed a more rigorous model that included the species equation with first-order, single-step decomposition kinetics. They also found that allowing for distributed reaction in the condensed phase could have a noticeable effect on the low-frequency thermal relaxation response. More recently, De Luca and Galfetti[8] considered the effects of distributed condensed phase reaction on dynamic burning and on stability, in particular. They found that distributed heat release in the high-temperature degradation layer helps static (linear) stability of super-rate burning in double-base propellant, but worsens dynamic (nonlinear) stability properties.

One purpose of this study was to investigate the applicability of large activation energy asymptotics in the condensed phase decomposition description (QSC assumption) for energetic solids by comparing numerical solutions for distributed condensed phase reaction with both numerical and analytical solutions assuming a surface reaction. Another purpose was to investigate the response in linear and nonlinear regimes using sine and pulse waveform inputs. Linear stability was also examined. As a limiting case to test the QSC assumption, condensed phase controlled burning (adiabatic gas) was considered. Condensed phase controlled burning may be considered an approximation of real burning under certain circumstances such as low pressure and radiation-augmented deflagration. Under these conditions the gas flame is far from the surface and gas phase conductive heat feedback becomes negligible. An additional motivation for considering the adiabatic gas case first is that simplified models for the gas phase reaction zone in burning solids have not been validated to the degree that simplified condensed phase reaction models have been. A relatively simple yet effective model of the condensed-phase reaction zone, single-step, zeroth-order decomposition, was assumed. (It has been shown elsewhere[1,20] that zeroth-order decomposition is a good condensed phase model for NC/NG propellants for both steady[1,20] and unsteady[1] burning, whereas the commonly assumed simple Arrhenius surface pyrolysis model is a poor one, especially for unsteady burning.[1]) Combustion was perturbed by a time-dependent radiant heat flux input. This allows the model to be used in conjunction with laser-augmented laboratory tests that are being developed to investigate the combustion mechanisms of solid propellants and energetic materials. Both sine waves and pulse waveforms of radiant heat flux input were used in the unsteady simulations. High accuracy was obtained using fourth-order compact finite differencing.

Modeling

Distributed Reaction Model

The less restrictive, distributed reaction (non-QSC) model is presented first and the more restrictive, surface reaction (QSC) model is presented afterward as a limiting case. The distributed reaction model allows for description of spatial distribution of chemical reaction in the condensed phase. Single-step decomposition of reactant (with mass fraction Y) going to product (mass fraction $1 - Y$) is assumed with activation energy E_c and overall exothermic heat release Q_c. (The initial decomposition step is presumably endothermic, often followed by rapid recombination reactions resulting in a net exothermic heat release.) The value of E_c is unrestricted (i.e., large activation energy is not required, although it is generally the case for realistic parameters). Spatial variations are assumed to occur in only one direction, normal to the solid surface; the origin of the x coordinate is attached to the burning surface with the positive coordinate into the gas phase. Density, thermal conductivity, and specific heat of the condensed phase are assumed constant in the governing equations that follow. (The term condensed phase is used to recognize that there will often be liquefaction of the solid near the surface; however, phase-change effects such as latent heats and property changes, which affect the response on the same order as the phenomenon being investigated, have not been included.) The conservation of mass equation is

$$\frac{\partial \rho_c}{\partial t} + \rho_c \frac{\partial r_b}{\partial x} = 0 \tag{1}$$

Since constant condensed phase density is assumed, the mass flux is independent of x,

$$m(t) = \rho_c r_b(t) \tag{2}$$

The species conservation equation is

$$\rho_c \frac{\partial Y}{\partial t} + m \frac{\partial Y}{\partial x} = -\Omega, \qquad Y(-\infty, t) = 1 \tag{3}$$

Diffusion of species in the condensed phase has been neglected, as is appropriate and customary. The rate of depletion [Eq. (4)] of unreacted solid with mass fraction Y, is assumed to be independent of Y (zeroth-order reaction):

$$\Omega = \rho_c A \exp[(-E_c)/RT] \tag{4}$$

The unsteady mass flux is then given by the integral of Eq. (3), assuming $Y(0, t) = 0$,

$$m(t) = \rho_c A \int_{-\infty}^{0} e^{-E_c/RT}\,dx + \rho_c \int_{-\infty}^{0} \frac{\partial Y}{\partial t}\,dx \tag{5}$$

The energy equation is

$$\rho_c C \frac{\partial T}{\partial t} + \rho_c C r_b \frac{\partial T}{\partial x} = k_c \frac{\partial^2 T}{\partial x^2} + Q_c \Omega + q K_a \exp(K_a x) \tag{6}$$

The energy equation includes accumulation, advection, conduction (diffusion), chemical source, and radiation absorption terms. The radiation absorption term is based on Beer's law for transport of a collimated incident radiative flux in an absorbing, nonemitting, nonscattering medium with constant absorption coefficient K_a. The upstream and surface boundary conditions are

$$T(-\infty, t) = T_0 \tag{7}$$

$$f_s = \left(\frac{\partial T}{\partial x}\right)_{s-} = \frac{k_g}{k_c}\left(\frac{\partial T}{\partial x}\right)_{s+} = f_s(r_b, T_s, p) \tag{8}$$

The surface boundary condition, Eq. (8), is an energy balance on the surface; the form shown in Eq. (8) ignores latent heat of evaporation and change in kinetic energy. In general, the surface temperature gradient f_s must be supplied by some model of the gas phase. For condensed phase controlled burning, an adiabatic gas is assumed; the temperature gradient on the gas side of the interface is zero. For distributed condensed phase reaction the temperature gradient on the condensed phase side of the interface is also zero, $f_s = 0$. (The chemical heat release occurs below, not at, the surface.)

This completes the formulation of the mathematical problem. Two differential equations (species and energy) are solved for two field variables $Y(x, t)$ and $T(x, t)$. However, since two boundary conditions are assumed for mass fraction, whereas the species equation is only first-order, we can anticipate that a solution will exist only for a unique burning rate. Thus, the instantaneous burning rate $r_b(t)$ [or mass flux $m(t)$] is an eigenvalue of the system of equations, to be determined using Eq. (5). In general, the solution of Eqs. (3–8) requires numerical methods for both unsteady [$q(t)$] and steady (q = const) conditions. However, an approximate steady-state analytical solution exists for the case of the large activation energy, $E_c/RT \to \infty$.

Steady-State Surface Reaction Solution

The condition $E_c/RT >> 1$ is satisfied to a good degree ($E_c/2RT_s > 5$) for most solid energetic materials. Under this approximation an inert convective–diffusive zone of length scale $x_c = \alpha_c/\overline{r_b}$ and time scale $t_c = x_c/\overline{r_b} = \alpha_c/\overline{r_b}^2$ develops, followed by a thin reactive–diffusive zone at the surface of length scale $x_R = x_c/(E_c/2R\overline{T_s})$ and time scale $t_R = x_R/\overline{r_b}$. It is assumed that a fraction of the radiant flux f_r is transmitted through the reactive–diffusive zone (i.e., absorbed below the reactive–diffusive zone), while the remainder $1 - f_r$ is absorbed in the reactive–diffusive zone (this assumption has been justified in Ref. 9). The energy equation [Eq. (6)] in the convective–diffusive zone becomes Eq. (17) (without the time-derivative term). The steady-temperature profile in the convective–diffusive zone is solved from the time-independent form of Eq. (17) using the matching condition $\bar{T} = \overline{T_s}$ at $x = 0$ to give

$$\bar{\theta}(\xi) = \{1 - [f_r J/(1 - \beta_r)]\}\exp(\xi) + [f_r J/(1 - \beta_r)]\exp(\beta_r \xi) \tag{9}$$

where

$$f_r = \exp[(-x_R)/x_r], \quad x_r = 1/K_a, \quad x_R = (\alpha_c/\overline{r_b})/(E_c/2R\overline{T_s}) \tag{10}$$

When x_r is much less than x_R, all of the radiation is absorbed in the surface reaction layer ($f_r = 0$). Conversely, when x_r is much greater than x_R, all of the radiation is absorbed below the surface reaction layer ($f_r = 1$).

The reactive–diffusive zone is analyzed using the time-independent form of Eq. (6) and ignoring the convective term. This, together with matching conditions, gives the result[10]:

$$\bar{m}^2 = \frac{A\overline{T}_s^2 \rho_c^2 C \alpha_c \exp[(-E_c)/R\overline{T_s}]}{E_c[C(\overline{T_s} - T_0) - (Q_c/2) - (f_r \bar{q}/\bar{m})]} \tag{11}$$

The steady solution is completed with the addition of the energy equation (integral) with the adiabatic gas condition:

$$\overline{T_s} = T_0 + (\bar{q}/\bar{m}C) + (Q_c/C) \tag{12}$$

Equations (11) and (12) represent the steady burning relations or laws, which may be written in the more general form:

$$f(\overline{r_b}, \overline{T_s}, T_0, \bar{p}, \bar{q}) = 0 \tag{13}$$

$$g(\overline{r_b}, \overline{T_s}, T_0, \bar{p}, \bar{q}) = 0 \tag{14}$$

To emphasize that burning rate and surface temperature are the dependent variables, and initial temperature, pressure, and absorbed radiant flux are the independent variables, these general relations may also be rewritten as,

$$\overline{r_b} = \overline{r_b}(T_0, \bar{p}, \bar{q}) \tag{15}$$

$$\overline{T_s} = \overline{T_s}(T_0, \bar{p}, \bar{q}) \tag{16}$$

which is a useful form for application of these results in the context of ZN theory.

Surface Reaction Model

The time-dependent QSC model is based on the phenomenological approach developed by Soviet researchers, especially Novozhilov,[11] and originated by Zeldovich in 1942. This theory has been called ZN theory, QSHOD theory, or the t_c approximation. It is based on the assumptions of QSG and QSC zones, homogeneous solid, and a one-dimensional flame (i.e., one-dimensional heat feedback). Thermal layer relaxation, with time scale t_c, is the only non-quasi-steady process. The condensed phase reaction layer and the gas phase region (if included) are considered to respond instantly to changing external conditions. The condensed phase reaction layer is approximated as infinitesimally thin; condensed phase reactions are confined to the interface between the unreacted condensed phase and the gas phase. Therefore, the temperature of the reaction layer is considered to be the surface temperature of the solid. This simplification is justified when the effective activation energy of the condensed phase decomposition is large enough that the reaction zone is very thin relative to the thermal layer thickness ($E_c/RT \to \infty$; $x_c >> x_R \to 0$). The question that has not been adequately addressed, at least for unsteady response, is the quantitative one: how large must the activation energy be for a given predictive accuracy? Values of $E_c/2RT_s$ for typical energetic solids are 5–15. For steady burning, it has been found that even the smallest realistic values (~5) are large enough that formulas based on activation energy asymptotics are accurate to within a few percent for burning rate. However, this does not guarantee similar accuracy for the surface reaction approximation in predicting unsteady burning.

The surface reaction approximation eliminates the need for solving the species equation. The mass fraction becomes a step function, $Y = 1$ in the condensed phase ($-\infty < x < 0$) and $Y = 0$ at $x = 0$. The unsteady energy equation in the condensed phase becomes

$$\rho_c C \frac{\partial T}{\partial t} + \rho_c C r_b \frac{\partial T}{\partial x} = k_c \frac{\partial^2 T}{\partial x^2} + f_r q K_a \exp(K_a x) \tag{17}$$

The term for heat release in the condensed phase from chemical reaction has been eliminated from the energy equation and included in the surface boundary condition, Eq. (19):

$$T(-\infty, t) = T_0 \tag{18}$$

$$f_s = \left(\frac{\partial T}{\partial x}\right)_{s-} = \frac{(1 - f_r)q}{k_c} + \frac{k_g}{k_c}\left(\frac{\partial T}{\partial x}\right)_{s+} + \frac{\rho_c r_b Q_c}{k_c} \tag{19}$$

The surface boundary condition also contains the radiant energy absorbed in the surface reaction zone. Similar to the distributed reaction model, the conductive heat flux from the gas phase is neglected, $(\partial T/\partial x)_{s+} = 0$. The transmissivity of the surface reaction layer is defined as before [Eq. (10)]. In general, it would be based on the instantaneous r_b and T_s values, although the case of constant f_r (based on the mean r_b and T_s values) was also considered.

Since the assumption of an infinitesimally thin reaction layer results in the elimination of the species equation, it would appear that a means for solving for unsteady mass flux has been eliminated. The ZN method provides a means to determine the unsteady mass flux. The ZN method demonstrates how a theory of nonsteady combustion can be developed without detailed knowledge of the combustion process, but only general steady-state burning information.

For steady-state burning, the propellant mass flux and surface temperature are given as functions of initial temperature, radiant heat flux, and pressure by the steady burning laws, Eqs. (15) and (16) or Eqs. (11) and (12), for the case considered here. The ZN method consists of transforming these functional relations using the integral energy equation

$$\bar{f}_s = (\bar{r}_b/\alpha_c)(\bar{T}_s - T_0) - (f_r\bar{q}/k_c) \tag{20}$$

to the following form by eliminating T_0:

$$\bar{m} = \bar{m}(\bar{f}_s, \bar{p}, \bar{q}) \tag{21}$$

$$\bar{T}_s = \bar{T}_s(\bar{f}_s, \bar{p}, \bar{q}) \tag{22}$$

These functional relations have been shown to be valid on a time-dependent basis[11] under the QSC and QSG assumptions, giving

$$m = m(f_s, p, q) \tag{23}$$

$$T_s = T_s(f_s, p, q) \tag{24}$$

Using the time-dependent integral energy equation (with $q_c = 0$) for surface reaction [for distributed reaction an additional term $-(1/r_b)(\partial/\partial t)\int_{-\infty}^{0}(YQ_c/C)\,dx$ appears on the right-hand side]:

$$T_s = T_0 - \frac{1}{r_b}\frac{\partial}{\partial t}\int_{-\infty}^{0} T\,dx + \frac{Q_c}{C} + \frac{q}{mC} \tag{25}$$

an apparent initial temperature T_{0a} can be defined

$$T_{0a} = T_0 - \frac{1}{r_b}\frac{\partial}{\partial t}\int_{-\infty}^{0} T\,dx \tag{26}$$

$$f_s = (r_b/\alpha_c)(T_s - T_{0a}) - (f_r q/k_c) \tag{27}$$

and the unsteady burning laws [Eqs. (23) and (24)] can be rewritten as

$$m = m(T_{0a}, p, q) \tag{28}$$

$$T_s = T_s(T_{0a}, p, q) \tag{29}$$

For the adiabatic gas case considered here, the steady burning relations [Eqs. (11) and (12)] become the following unsteady relations:

$$m^2 = \frac{ART_s^2\rho_c^2 C\alpha_c \exp(-E_c/RT_s)}{E_c\{(Q_c/2) + [(1 - f_r)q/m]\}} \tag{30}$$

$$T_{0a} = T_s - (Q_c/C) - (q/mC) \tag{31}$$

Hence, the ZN method provides a means to determine unsteady mass flux for the assumption of an infinitesimally thin reaction layer. The surface reaction (QSC) model [Eqs. (17–19) and (30)] and the distributed reaction (non-QSC) model [Eqs. (3–8)] were both solved numerically using explicit fourth-order compact differencing.

Quasisteady Linearized Analytical Solution

For the surface reaction (QSC) model, an analytical solution for the combustion response is available in the linear approximation ($\Delta m << \bar{m}$). The response function for arbitrary (but quasisteady) gas flame and surface pyrolysis processes can be obtained[12] solving Eqs. (17), (18), and (20) in the linear approximation:

$$R_q = \frac{\nu_q + \delta_q(\lambda - 1) - [kf_r J(\lambda - 1)/(\beta_r + \lambda - 1)]}{\lambda r + k/\lambda - (r + k) + 1 - [kf_r J(\lambda - 1)/\lambda(\beta_r + \lambda - 1)]} \tag{32}$$

Equation (32) assumes f_r (the surface reaction layer transmissivity) is a constant parameter. The steady-state sensitivity parameters, ν_q, δ_q, r, and k, were obtained from the steady-state burning laws [Eqs. (11) and (12)] assuming constant f_r:

$$\nu_q = \left(\frac{\partial\, \ell n\, \bar{m}}{\partial\, \ell n\, \bar{q}}\right)_{T_0,p} = \left(1 + \frac{2}{\left(\frac{\bar{q}}{\bar{m}C\bar{T}_s}\right)\left\{2 + \frac{E_c}{R\bar{T}_s} - \frac{(1 - f_r)}{(Q_c/2C\bar{T}_s) + [(1 - f_r)\bar{q}/\bar{m}C\bar{T}_s]}\right\}}\right)^{-1} \tag{33}$$

$$k = (\bar{T}_s - T_0)\left(\frac{\partial\, \ell n\, \bar{m}}{\partial T_0}\right)_{q,p} = \frac{\frac{1}{\bar{T}_s}\left(2 + \frac{E_c}{R\bar{T}_s}\right)(\bar{T}_s - T_0)}{2 + \frac{\bar{q}[2 + (E_c/R\bar{T}_s)]}{\bar{m}C\bar{T}_s} - \left[\frac{Q_c\bar{m}}{2(1 - f_r)\bar{q}} + 1\right]^{-1}} \tag{34}$$

$$r = \left(\frac{\partial \bar{T}_s}{\partial T_0}\right)_{q,p} = \left(1 - \frac{2 + \frac{E_c}{R\bar{T}_s}}{\left\{\frac{1}{(\bar{q}/\bar{m}C\bar{T}_s) + [Q_c/2C\bar{T}_s(1 - f_r)]} - \frac{2\bar{m}C\bar{T}_s}{\bar{q}}\right\}}\right)^{-1} \tag{35}$$

$$\delta_q = \nu_q r - \mu_q k = n_q r \tag{36}$$

where

$$n_q = \left(\frac{\partial\, \ell n\, \bar{m}}{\partial\, \ell n\, \bar{q}}\right)_{\bar{T}_s,p} = \left[-1 - \frac{\bar{m}Q_c}{(1 - f_r)\bar{q}}\right]^{-1} \tag{37}$$

Results

Steady-State Results

A set of baseline parameters was selected to be representative of energetic solids in general: $E_c = 20$ kcal/mole, $A = 2$

Table 1 Steady-state results for baseline case, E_c = 20 and 40 kcal/mole

	Surface reaction		Distributed reaction
E_c, kcal/mole	Analytical	Numerical	Numerical
E_c = 20			
$\bar{r}_b$, cm/s	0.305	0.305	0.307
$\bar{T}_s$, K	913.5	913.4	911.5
E_c = 40			
$\bar{r}_b$, cm/s	0.0900	0.0897	0.0918
$\bar{T}_s$, K	1586	1586	1564

$\times 10^7$ s^{-1}, Q_c = 100 cal/g, ρ_c = 1.95 g/cm^3, α_c = 0.001 cm^2/s, C = 0.3 cal/g-K, K_a = 1000 cm^{-1}, $\bar{q}$ = 50 cal/cm^2-s, and T_0 = 300 K. These parameters correspond approximately to radiation-augmented ammonium perchlorate combustion, although the intent was not to match AP. Except for variations in K_a, E_c, and $\bar{q}$, these input parameters were used for all of the numerical tests discussed in this article. Table 1 compares numerical predictions to analytical predictions for steady-state (constant radiant flux) burning rate and surface temperature for the baseline case (E_c = 20 kcal/mole) and for E_c = 40 kcal/mole.

The baseline (E_c = 20) results for burning rate and surface temperature are realistic for a material like AP. The E_c = 40 results are not as realistic (surface temperature is too high) but were conducted for comparison of numerical and analytical predictions and are also included. The dimensionless activation energy ($E_c/2R\bar{T}_s$) was 5.5 and 6.5 for the E_c = 20 and 40 cases, respectively, large enough for good agreement between steady-state surface reaction and distributed reaction results. The surface reaction formulations (analytical and numerical) gave steady burning rates and surface temperatures within 2% of the corresponding distributed reaction values. The steady-state parameters for the baseline case for surface reaction from Eqs. (10) and (33–37) are: ν_q = 0.640, δ_q = −0.077, r = 0.282, k = 1.57, f_r = 0.552, and J = 0.457.

Although the distributed reaction and surface reaction models gave almost identical results for steady burning rate and surface temperature, the resulting temperature profiles are quite different near the surface, as shown in Fig. 1. The distributed reaction profile maintains a zero surface temperature gradient since conductive heat flux from the gas phase is neglected, whereas the surface reaction profile has a nonzero gradient. The surface gradient for the surface reaction model is because of chemical heat release and radiative energy absorbed in the surface reaction zone. The unreacted solid mass fraction profile and normalized reaction rate for the distributed reaction case are also shown in Fig. 1. The reaction zone is confined to a region <20 μm in thickness near the surface (the scaling estimate $x_R = x_c/(E_c/2R\bar{T}_s)$ gives a value of 6 μm).

Linear Stability of Steady-State Burning

Linear stability of the considered system was investigated for the surface reaction case. Novozhilov[13] solved for stability criteria assuming $\bar{q} = 0$. Later, Son et al.[14] investigated stability for $\bar{q} \neq 0$ and arbitrary absorption coefficient, but particularly the limits of surface absorption and in-depth absorption. In this study the stability of the surface reaction model was investigated in greater detail for an arbitrary reaction layer transmissivity. The stability criterion is a nonlinear relationship between the r and k sensitivity parameters, which must be solved by iteration.[15]

Figure 2 presents the stability boundaries for the baseline case and several variations. The limiting cases of an opaque propellant ($K_a \to \infty$, $x_r << x_R$, $f_r \to 0$) and a transparent propellant ($K_a \to 0$, $x_r >> x_c$, $f_r \to 1$) form an envelope of space within which the intermediate opacity cases fall. [Note that $x_r >> x_R$ is sufficient for $f_r \to 1$, that is only the reaction layer need be optically thin. However, the limit being considered here is that the heated layer x_c ($>>x_R$) is also optically thin, which is more severe.) For the transparent limit (K_a < 10 cm^{-1} is sufficiently small for the baseline parameters] the stability boundary depends on the flux J; two transparent cases are shown, $\bar{q}$ = 5 cal/cm^2-s (J = 0.233) and $\bar{q}$ = 50 cal/cm^2-s (J = 0.434). As $\bar{q}$ increases from 5 to 50 cal/cm^2-s, the stable region decreases in r-k space. However, it is important to note that this does not mean that the effect of increasing mean radiant flux is necessarily that of destabilizing the system. System stability also depends on how the actual operating r and k values of the system vary with mean flux. For the condensed phase controlled system considered here, it was found, as discussed later, that the effect of increasing mean flux on the parameters (k in particular) was to promote stability of the system.

The stability boundary for the baseline case ($\bar{q}$ = 50 cal/cm^2-s, K_a = 1000 cm^{-1}, f_r = 0.552) is seen to fall between the opaque and transparent limits in Fig. 2. The actual r-k operating values for the baseline case (r = 0.2823 and k = 1.5720) are indicated by the diamond symbol and show that the baseline case is linearly stable. Numerical results showed that for the baseline case the distributed reaction model was also stable (recall that this analysis is based on the quasisteady surface reaction model).

The effect of mean flux on stability was examined by reducing the mean flux from 50 to 5 cal/cm^2-s. The effect on the stability boundary is to shift it to the right in Fig. 2 (increasing the stable region in r-k space) as discussed previously for the

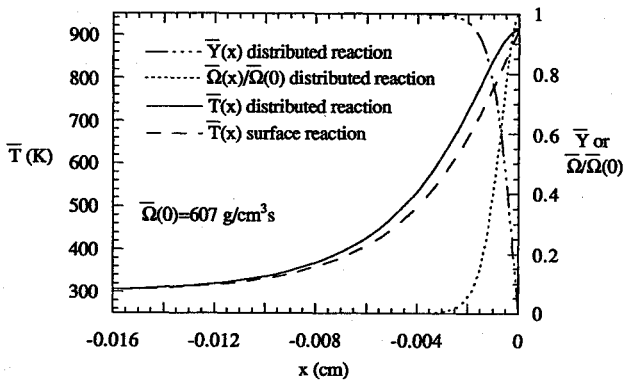

Fig. 1 Steady temperature, mass fraction, and reaction rate profiles for baseline case (E_c = 20 kcal/mole, $A = 2 \times 10^7$ s^{-1}, Q_c = 100 cal/g, ρ_c = 1.95 g/cm^3, α_c = 0.001 cal/g, C = 0.3 cal/g-K, K_a = 1000 cm^{-1}, $\bar{q}$ = 50 cal/cm^2-s, and T_0 = 300 K).

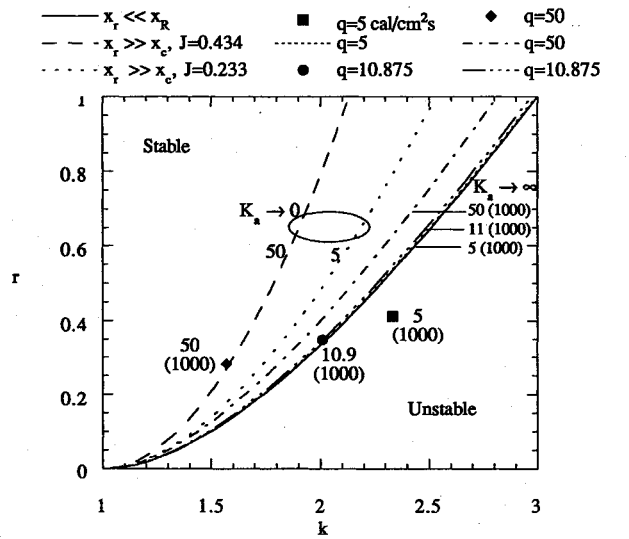

Fig. 2 Stability boundaries and operating points. Numbers indicate absorbed flux $\bar{q}$ in cal/cm^2-s and (in parentheses) absorption coefficient K_a in cm^{-1}.

transparent limit. (The $\bar{q}$ = 5 cal/cm^2-s case is almost indistinguishable from the opaque limit because for K_a = 1000 cm^{-1} the reaction layer transmissivity f_r = 0.064 is so small.) The effect on the k parameter is to increase from 1.572 (for 50 cal/cm^2-s) to 2.334 (for 5 cal/cm^2-s). This increase in k shifts the system into the unstable region (square symbol).

These results demonstrate that a value for radiant heat flux exists between 5–50 cal/cm^2-s, where the operating point is located on the stability boundary. This point can be calculated by solving the steady-state surface reaction model equations for mass flux [Eq. (11)], energy [Eq. (12)], and sensitivity parameters [Eqs. (33–37)] with the stability criterion equation. This point was found to occur at $\bar{q}$ = 10.875 cal/cm^2-s with f_r = 0.258. Since f_r is small, this stability boundary is also close to the surface absorption limit.

An interesting observation relative to double-base propellant combustion can be made by substituting relevant parameters into the present model. (An adiabatic gas condition might be considered a rough, first approximation, since studies have shown that below 100 atm the conductive heat feedback is small, although probably not negligibly so, compared to the condensed phase heat release in NC/NG systems.[1]) The following parameters were altered from the baseline values: $\bar{q}$ = 5 cal/cm^2-s, A = 1e17 s^{-1}, E_c = 40 kcal/mole, Q_c = 100 cal/g, K_a = 1000 cm^{-1}, and ρ_c = 1.6 g/cm^3. The analytical steady results for this system are $\overline{r_b}$ = 0.311 cm/s and $\overline{T_s}$ = 614 K. This increases the nondimensional activation energy to $E_c/2R\overline{T_s}$ = 16.4. For these conditions the sensitivity parameters are r = 0.5446 and k = 4.945. This value of temperature sensitivity parameter k is very high. It is apparent from the r-k values that the system is unstable (Fig. 2), even though a steady-state solution exists. For this case both numerical codes (surface and distributed reaction) exhibited unstable behavior. Other parameter variations were investigated, but a set of stable, realistic double-base parameters was not found for the adiabatic gas model. Usually k was too large. It has been noted[16] that this intrinsic instability associated with the high activation energy condensed phase controlled system may be eliminated by gas phase conductive heat feedback. Even a small (relative to the condensed phase heat release) amount of gas phase heat feedback appears to be responsible for linear stability in what would otherwise be an intrinsically unstable system.

No stability investigation was attempted for the distributed reaction model. For the conditions considered in this study the distributed reaction model was found to be either stable or unstable according to the behavior of the surface reaction model. It is acknowledged, however, that distributed reaction could have an impact on stability, as discussed by De Luca and Galfetti.[8]

Quasisteady Linear Response

The QSC linear response function is given in Figs. 3 (magnitude) and 4 (phase) for the baseline case. The constant f_r analytical solution [Eq. (32)] is shown by the solid lines. As seen in Fig. 3, the response magnitude peaks at approximately 60 Hz (the scaling estimate from $t_c = x_c/\overline{r_b} = \alpha_c/\overline{r}_b^2$ is 93 Hz). At this frequency the period of the disturbance is approximately the same as the period or residence time of material in the heated layer t_c; the burning rate and radiant heat flux are in phase as indicated by the zero crossing in Fig. 4. The burning rate leads the radiant heat flux input at frequencies below the peak and lags above.

Numerical results for the QSC linear response are also presented in Figs. 3 and 4. Any numerical simulation of transient homogeneous propellant combustion should be able to match the analytic solution in the linearized, quasisteady limit. Such comparison is an important step in validating the numerical simulation. In this study numerical validation in the linearized, quasisteady limit was conducted using both pulse and sine wave inputs. The sine inputs had an amplitude of Δq = 1 cal/cm^2-s, with a mean heat flux of $\bar{q}$ = 50 cal/cm^2-s, and frequencies ranging from 40 to 600 Hz. The results for the constant f_r numerical-surface reaction model are shown in Figs. 3 and 4 (× symbols). The numerical results match the analytical results as they should. Linearity of the numerical calculations was verified by changing the sine wave input amplitude and receiving the same response function. Grid independence was also verified. Periodic pulse inputs (pulse trains) were also investigated numerically. The output for these cases was spectrally analyzed [fast Fourier transform (FFT)] and gave the same response for sufficiently small pulse amplitudes (<1 cal/cm^2-s).

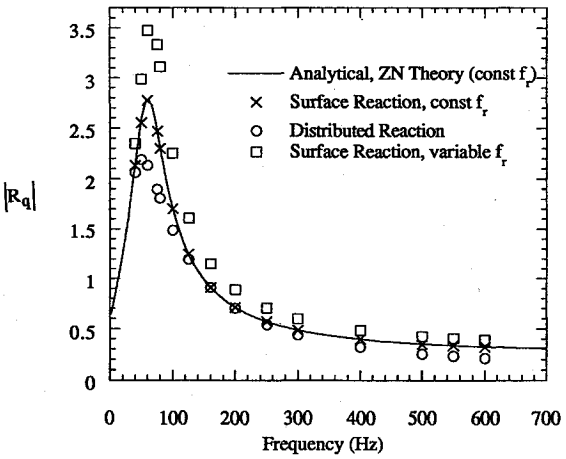

Fig. 3 Magnitude of linear response function for baseline case.

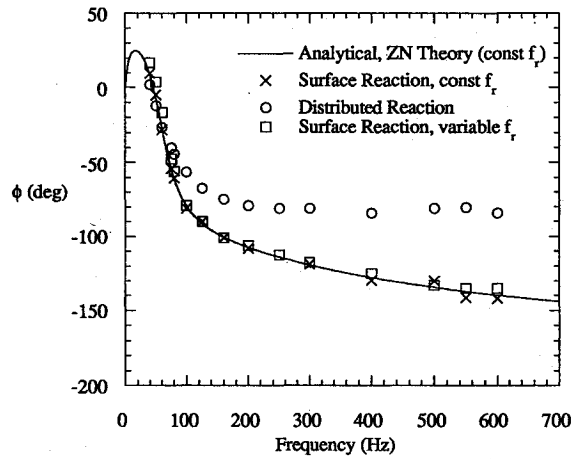

Fig. 4 Phase angle of linear response function for baseline case.

The numerical simulation was also tested at a higher activation energy (E_c = 40 kcal/mole) and over a range of absorption coefficients (100–10,000 cm^{-1}). The sinusoidal input frequency was 50 Hz with an amplitude of Δq = 1 cal/cm^2-s. As seen in Table 2, the numerically calculated response (constant f_r) matches the analytical response. Good agreement was obtained between numerical and analytical predictions for QSC (surface reaction) response over a range of absorption coefficients, high- and low-activation energies, and for all frequencies. Again, these results (E_c = 40) are included, not because they simulate any real material necessarily, but mostly because they demonstrate agreement between the numerical simulation and a closed-form analytic solution, and this agreement is necessary for validating and establishing confidence in the numerical representation.

The previous results were based on the assumption that f_r was a constant parameter [see discussion following Eq. (19)]. The results for variable f_r for the baseline case are shown in Figs. 3 and 4 (square symbols). The largest deviation from the

Table 2 Quasisteady linear response function for E_c = 40 kcal/mole at f = 50 Hz

		Analytical, f_r = const		Numerical, f_r = const		Numerical, $f_r \neq$ const	
K_a, 1/cm	f_r	$\lvert R_q \rvert$	ϕ, deg	$\lvert R_q \rvert$	ϕ, deg	$\lvert R_q \rvert$	ϕ, deg
100	0.8632	0.360	−134.4	0.359	−134.1	0.454	−135.0
400	0.5183	0.853	−104.4	0.860	−103.5	1.158	−99.0
750	0.2739	1.004	−91.3	1.008	−90.0	1.263	−86.9
1,000	0.1727	1.033	−87.8	1.034	−88.0	1.249	−85.5
10,000	0	1.050	−84.7	1.056	−85.0	1.056	−83.7

constant f_r case is in the magnitude; phase is relatively unaffected. Comparisons were also made for the higher activation energy case (40 kcal/mole) over a range of absorption coefficients as shown in Table 2. As in Fig. 3, the results of Table 2 show that the magnitude of the response $|R_q|$ is greater when f_r is allowed to vary. The relative difference in R_q between constant f_r and variable f_r is greatest for intermediate values ($f_r \sim 0.5$). This is because for either the opaque ($f_r = 0$) or translucent ($f_r = 1$) limits, the value of f_r becomes insensitive to r_b and T_s, and the distinction between variable and constant f_r becomes irrelevant.

Non-Quasi-Steady Linear Response

To investigate the effect of the QSC assumption on linear response, the distributed reaction (non-QSC) model was exercised and the predictions compared with those of the surface reaction model for the baseline case. The results are shown in Figs. 3 and 4 as circle symbols. Figure 3 shows that the distributed reaction response magnitude is lower than both of the surface reaction responses, particularly near the peak. Since the constant f_r quasisteady response is closer to the exact distributed response, this may be taken as an indication that constant f_r is a better assumption for the QSC approach, at least for this set of parameters. Even so, the QSC assumption overpredicts $|R_q|$ by 30% near the peak. The response phase also exhibits significant deviation. Figure 4 shows that at frequencies above 100 Hz, the quasisteady assumption significantly overpredicts the amount of phase lag. An estimate of the frequency at which the QSC assumption should begin to break down can be obtained from $t_R = x_R/\overline{r_b} = t_c/(E_c/2R\overline{T_s})$ as $f_R = 1/t_R = 512$ Hz. Thus, the non-QSC results show that the QSC model exhibits significant error (30%) in response magnitude, even at frequencies well below f_R, and that at frequencies as low as one-fourth f_R (100–120 Hz in the present calculations) the phase is beginning the deviate significantly. The error in phase can be seen to get progressively worse with increasing frequency; the phase evidently will not recover as frequency becomes very high (where additional error because of the QSG assumption will begin to enter). The fundamental reason for the response difference between the surface reaction (QSC) and distributed reaction (non-QSC) cases is the difference in their temperature profiles. As seen in Fig. 1, the two cases have significantly different profiles (gradients) near the surface, even though $\bar{T}_s$ is essentially the same. This difference has a significant effect on the unsteady response, as seen in Figs. 3 and 4.

There are two important implications of these findings. One is that for realistic energetic material properties, the effective condensed phase activation energy is usually large enough that an activation energy asymptotic description (which for steady state doesn't have to be, but can be, thought of as a surface reaction description), accurately predicts the primary steady dependent variables, namely, $\bar{r}_b$ and $\bar{T}_s$. However, if the surface reaction assumption is extended to time-dependent behavior (i.e., QSC assumption) for the same parameters, the high activation energy (surface reaction) description is not nearly as accurate. Apparently, the criterion for application of activation energy asymptotics is more severe for unsteady than steady burning. A second important implication is that breakdown of the QSC assumption will occur at lower frequencies and with greater consequence than has been expected. Graphic evidence of this can be seen in Fig. 4, which shows that if the response was taken to be the pressure-coupled response (just for the sake of illustration), in the 300–600 Hz range, the QSC model would predict acoustic damping by the combustion response, whereas the non-QSC model predicts negligible or only slight positive in-phase response.

It can be argued that the first conclusion above about accuracy of AEA in steady vs unsteady burning (which has been based on a condensed phase reaction model), might be extended to the gas phase flame zone and to conditions where at least partial control of the burning rate by gas phase reaction occurs. Activation energy asymptotics have been applied to the gas phase reaction zone, giving formulas[10] similar to Eq. (11). It is reasonable to expect such formulas to be much less accurate in their description of unsteady burning than steady burning. For example, for a gas phase dimensionless activation energy of 10, the steady burning rate predicted by AEA would probably be accurate to within a few percent whereas the linear response function predicted by activation energy asymptotics (AEA) (i.e., QSHOD theory) would probably not be better than 20–30% accurate. The fundamental reason, as stated previously, is that the temperature gradient, which is critical for unsteady calculations, is not as well represented by AEA as the temperature itself. Support for this argument can be found from two studies, which relaxed the QSG assumption, but retained the QSC assumption. Tien[2] used numerical methods that allow arbitrary gas phase activation energy, and Clavin and Lazimi[3] used AEA analysis that assumes large gas phase activation energy (see Fig. 9 of Ref. 3). At low pressure ($\rho_c/\rho_g = 1000$), where the condensed and gas phase thermal response peaks are widely separated in frequency, the low-frequency (condensed phase thermal) peak was nearly identical between the two AEA models [non-QSG (Ref. 3) and QSG]; however, Tien's numerical model ($E_g/RT_g = 10$) differed significantly. The explanation that a nondimensional activation energy of 10 isn't big enough seemed[3] "not entirely satisfactory for justifying such a large difference." The results presented here suggest otherwise: a nondimensional activation energy of 10 may be large enough to expect a few percent accuracy from AEA for steady burning rate, but not for unsteady burning rate.

The results of Figs. 3 and 4 showing the error associated with the QSC assumption for the adiabatic gas case suggest that a similar comparison should be done including conductive heat feedback from a gas flame. Limited calculations have been done using the gas-phase controlled burning AEA model of Williams[10] and these are discussed in Ref. 17. The essential results are the same, that at $f \sim f_R/4$ the response begins to deviate from the QSC model. Further investigation including gas phase effects is needed.

Nonlinear Response

Nonlinear behavior was investigated by using large amplitude sine and pulse inputs. Even though the usual definition of response function is not applicable to a nonlinear system, the linear definition was applied to the nonlinear case by spectrally decomposing (using FFT) the periodic output and assuming a linear response. For a sine wave input at f, the output is

periodic with components at f, $2f$, $3f$, . . . , etc. The response for large amplitude sine inputs was calculated as if the system was linear and the output component at f was the only component. For periodic pulse inputs, the input contains frequency components at the pulse frequency f and the harmonics, $2f$, $3f$, . . . , etc. The input at f can produce output at $2f$, $3f$, $4f$, . . . , etc. The input at $2f$ can produce output at $2f$, $4f$, $6f$, . . . , etc. Thus, the output at any given frequency can result from the input at that frequency, or possibly some higher frequency. The response was calculated assuming the output at any given frequency was caused by the input at that frequency only. (This simulates what is sometimes done experimentally when a pulse input, preferably of small amplitude, is used to excite multiple frequencies and the data are spectrally analyzed assuming a linear response.) All of the nonlinear results presented here are for the baseline case parameters (mean heat flux of 50 cal/cm^2-s). Both surface (constant f_s) and distributed reaction models were tested.

Sine input results for the surface reaction model are shown in Figs. 5 and 6. The amplitude of the input heat flux is 50 cal/cm^2-s, the same as the mean heat flux. The response is quite linear for frequencies above 200 Hz. However, for frequencies near the peak (60 Hz) a significant portion of the response is being shifted to higher harmonics as indicated by the reduction in magnitude, from 2.8 to 1.3 at the peak.

Pulse input results for the surface reaction model are shown in Figs. 7 and 8. The amplitude of the input heat flux pulses was varied from 2 to 100 cal/cm^2-s (only the 12.5–100 cases are shown, however). The frequency of the pulses, 50 Hz, and pulse width, 2e-3 s, were held constant. For small pulse amplitudes (<5 cal/cm^2-s), the calculated response function approaches the linear response (more so for smaller amplitudes). As pulse amplitude increases, the calculated response deviates more from the linear response. Near the 60-Hz thermal conduction peak, the calculated response magnitude decreases below the linear response as pulse amplitude increases. This indicates that response is being shifted away from the 50-Hz input to higher frequencies, as was also seen in the sine tests (Fig. 5). At frequencies above 100 Hz, the calculated response magnitude is generally higher than the linear response, more so for larger pulse amplitudes. In particular, a secondary peak forms near 450 Hz and a third forms near 900 Hz, both of which are absent in the linear response.

The secondary peak at 450 Hz might be thought attributable to a condensed phase reaction layer response, since the characteristic frequency for the condensed phase reaction layer is 512 Hz. Such secondary peaks have been observed in laser-recoil response measurements.[18,19] However, this assignment is inconsistent with both the inertialess surface reaction assumption that was used in these calculations and with the absence of a peak near 450 Hz for the large amplitude sine input simulations (Fig. 5).

The reason for the second and third peaks seen in Fig. 7 probably has to do with the spectral content of the input signal. The sine waves that make up the input pulse train have maximum amplitude at the pulse frequency f; as frequency increases amplitude decreases monotonically to a local minimum

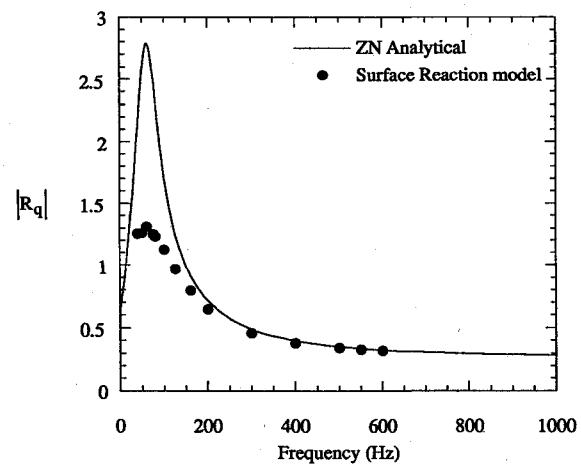

Fig. 5 Response magnitude for large amplitude (Δq = 50 cal/cm^2-s) sine input.

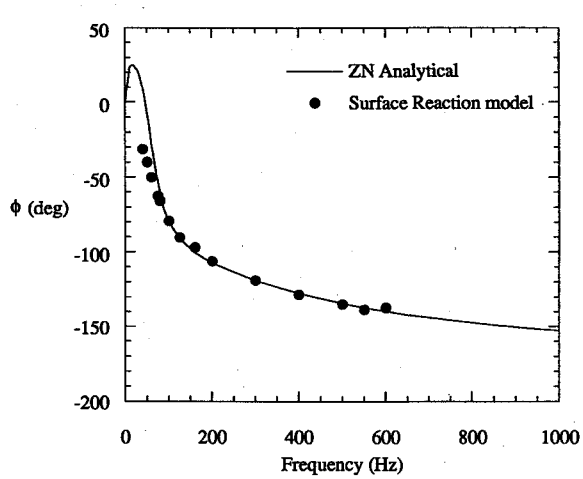

Fig. 6 Response phase angle for large amplitude (Δq = 50 cal/cm^2-s) sine input.

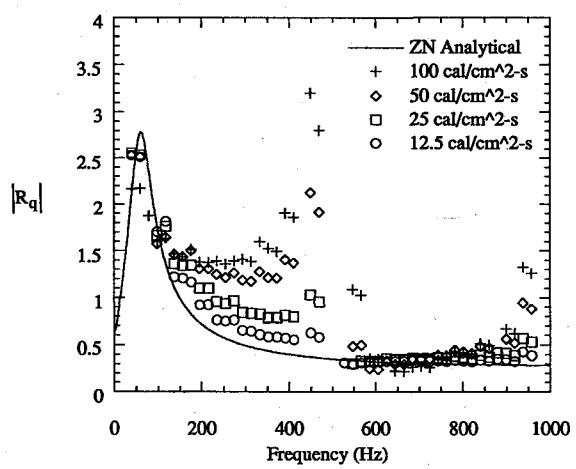

Fig. 7 Response magnitude for large amplitude pulse input; effect of pulse amplitude (surface reaction model, t_{pw} = 2e-3 s, f = 50 Hz).

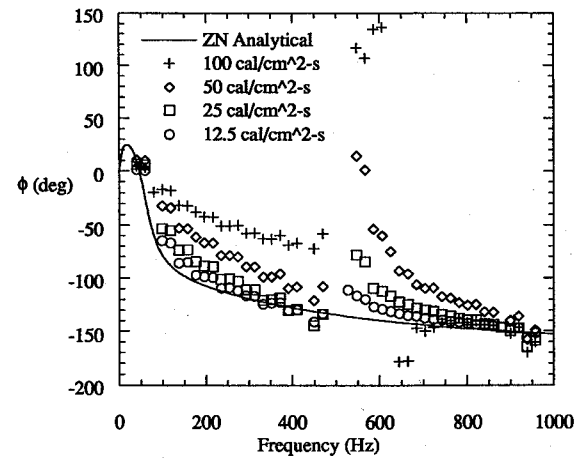

Fig. 8 Response phase angle for large amplitude pulse input; effect of pulse amplitude (surface reaction model, t_{pw} = 2e-3 s, f = 50 Hz).

at the frequency of the inverse pulse width, $1/t_{pw}$; then amplitude increases and decreases again to another local minimum at $2/t_{pw}$, etc. The frequency of the secondary peak, 450 Hz, corresponds closely to the inverse pulse width, $1/t_{pw}$ = 500 Hz. Since the response function is calculated assuming linearity, i.e., the output at 450 Hz is all because of input at 450 Hz, the input used in calculating R_q at 450 Hz is very small. The output at 450 Hz, however, is augmented by the high-frequency harmonics resulting from lower frequency Fourier components of the input. Therefore the indicated peaks at 450 and 900 Hz are probably because of nonlinear output at higher harmonics generated by lower frequency input.

Nonlinearity was also manifested in the mean burning rate for the pulse tests of Figs. 7 and 8. For amplitudes less than 5 cal/cm^2-s, there was less than 0.1% difference between the mean burning rate and the linear (constant flux) value. For amplitudes greater than 5 cal/cm^2-s, the mean burning rate decreased noticeably from the linear value as the pulse amplitude increased. For a pulse input with a frequency of 50 Hz and an amplitude of 50 cal/cm^2-s, the percent difference between mean burning rate and the linear value was 4.35%. For a pulse

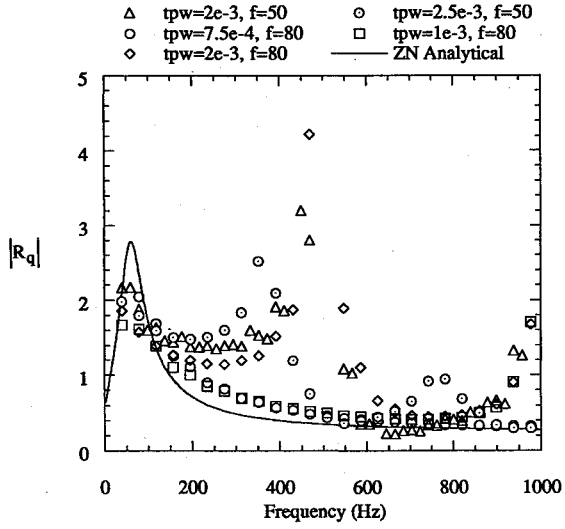

Fig. 9 Response magnitude for large amplitude pulse input; effect of pulse width and frequency (surface reaction model, Δq = 100 cal/cm^2-s).

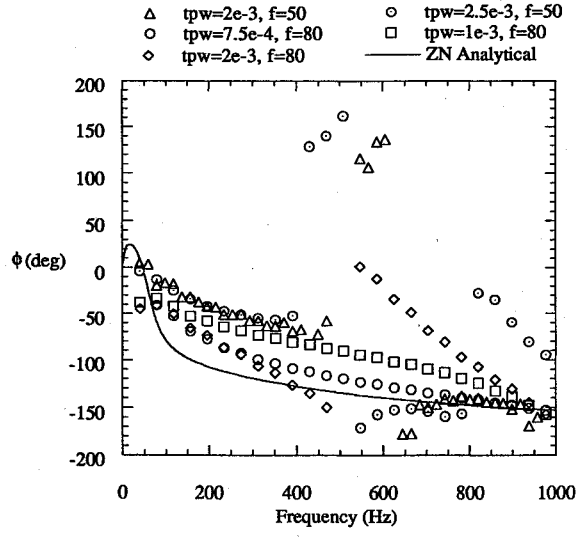

Fig. 10 Response phase angle for large amplitude pulse input; effect of pulse width and frequency (surface reaction model, Δq = 100 cal/cm^2-s).

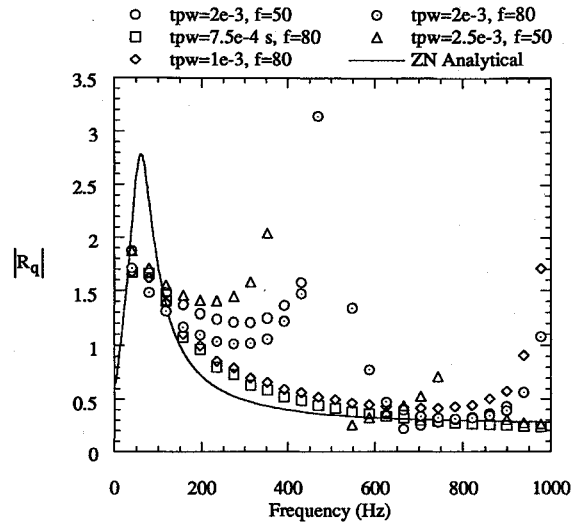

Fig. 11 Response magnitude for large amplitude pulse input; effect of pulse width and frequency (distributed reaction model, Δq = 100 cal/cm^2-s).

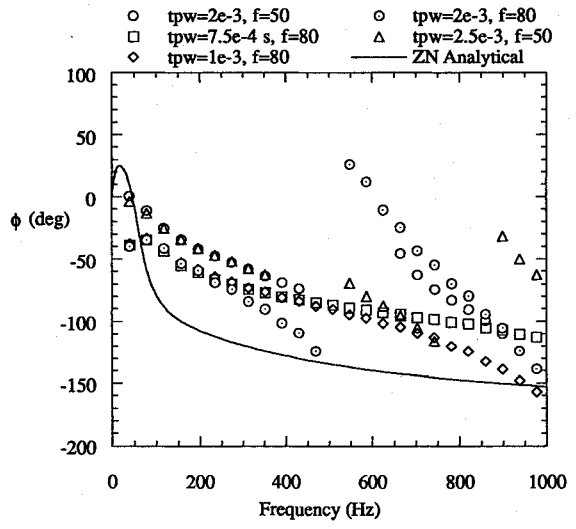

Fig. 12 Response phase angle for large amplitude pulse input; effect of pulse width and frequency (distributed reaction model, Δq = 100 cal/cm^2-s).

amplitude of 100 cal/cm^2-s, the percent difference increased to 12.9%.

Simulations conducted with variations in pulse width and pulse frequency verify the preceding explanation for the high-frequency nonlinear response peaks. Figures 9 and 10 show the calculated response for Δq = 100 cal/cm^2-s, t_{pw} ranging from 7.5e-4 s to 2.5e-3 s, and pulse frequencies of 50 and 80 Hz. In each case, where a peak would be expected at $1/t_{pw}$, $2/t_{pw}$, etc., a peak appeared. Pulse frequency had only a minor effect, as shown by the results for t_{pw} = 2e-3 s and frequencies of 50 and 80 Hz.

The simulations described previously for the surface reaction case were also performed for distributed reaction. The same general trends were observed in both cases. Figures 11 and 12 show the distributed reaction results for pulse input with Δq = 100 cal/cm^2-s, t_{pw} ranging from 7.5e-4 s to 2.5e-3 s, and pulse frequencies of 50 and 80 Hz (the distributed reaction analog of Figs. 9 and 10). The responses show multiple peaks: a low-frequency thermal relaxation peak, a secondary peak at $1/t_{pw}$, and multiple peaks thereafter, which are harmonics of the second peak. The magnitude of the responses was the main difference between the two models.

Conclusions

Comparison of surface and distributed reaction models for condensed phase controlled burning raises questions about the accuracy of the high activation energy, quasisteady reaction assumption in the condensed phase. While typical condensed phase activation energies ($E_c/2RT_s > 5$) are large enough for accurate (within 2%) prediction of steady burning rate and surface temperature by activation energy asymptotics, the criterion for comparable accuracy in predicting unsteady burning rate (e.g., linear response function) appears to be much more stringent. For typical condensed phase properties, the error in linear response magnitude because of the QSC assumption is as large as 30% at the thermal relaxation peak. Error in the response phase becomes noticeable at frequencies as low as one-fourth the characteristic condensed phase reaction layer frequency and approaches 60% as the frequency approaches the characteristic condensed phase reaction layer frequency. These results confirm what has been suggested by earlier studies, that condensed phase reaction layer inertia may play a significant role in the combustion response of energetic solids. They also suggest that at moderate pressures condensed-phase, reaction-layer inertia should be included before (at lower frequencies than), or at least in conjunction with, gas-phase inertia. Further consideration of non-quasi-steady condensed phase reaction effects is needed, particularly for pressure-driven unsteadiness, including gas phase conductive heat feedback.

Nonlinear response was also investigated. The primary effect of nonlinearity was to convert low-frequency response to higher frequencies. One interesting consequence of this behavior is that if pulsed test data, which are of sufficient amplitude to excite a nonlinear response, are spectrally analyzed assuming linearity, a multiple-peaked response function is obtained, with the frequency of the higher peaks correlating with pulse width. This observation is significant because secondary response peaks have been observed in pulsed laser-recoil experiments. Note, however, that not all secondary peaks are necessarily because of a nonlinear response. Violation of QSHOD assumptions can also result in secondary linear response peaks. The data of Ref. 18, in particular, which exhibited a secondary peak, were verified to be linear and must therefore be because of some real physical effect that violates QSHOD assumptions.

Finally, note that no suggestion is being made here that thermal radiation is an important coupling mechanism in combustion instability in solid rocket motors (it may or may not be). Pressure fluctuation is probably the most important coupling mechanism in most circumstances. What is at issue is not the type of disturbance driving the unsteadiness, it is the accuracy of activation energy asymptotics analysis in modeling such processes. The results of this article call into question widely accepted assumptions in that regard. If the QSC (surface reaction) assumption introduces a significant degree of error in radiation-driven unsteady burning rate predictions, it can easily do the same for pressure-driven unsteady burning.[17] The key is not the driving mechanism, but the error in the temperature profile. That error can carry over to pressure-driven unsteady burning.[17]

Acknowledgments

The financial support of the Office of Naval Research, N00014-91-J-1977, and National Science Foundation, CTS 91-13151, is gratefully acknowledged. Many of the ideas considered here were suggested by Steve Son of Los Alamos National Laboratory, who also did the initial code development.

References

[1]Brewster, M. Q., and Son, S. F., "Quasi-Steady Combustion Modeling of Homogeneous Solid Propellants," *Combustion and Flame*, Vol. 103, 1995, pp. 11–26.

[2]Tien, J. S., "Oscillatory Burning of Solid Propellants Including Gas Phase Time Lag," *Combustion Science and Technology*, Vol. 5, 1972, pp. 47–54.

[3]Clavin, P., and Lazimi, D., "Theoretical Analysis of Oscillatory Burning of Homogeneous Solid Propellant Including Non-Steady Gas Phase Effects," *Combustion Science and Technology*, Vol. 83, 1992, pp. 1–32.

[4]Kuo, K. K., Gore, J. P., and Summerfield, M., "Transient Burning of Solid Propellants," *Fundamentals of Solid Propellant Combustion*, edited by K. K. Kuo and M. Summerfield, Vol. 90, Progress in Astronautics and Aeronautics, AIAA, New York, 1984, Chap. 11.

[5]Culick, F. E. C., "Calculation of the Admittance Function for a Burning Surface," *Astronautica Acta*, Vol. 13, 1967, pp. 221–237.

[6]Williams, F. A., "Quasi-Steady Gas-Phase Flame Theory in Unsteady Burning of a Homogeneous Solid Propellant," *AIAA Journal*, Vol. 11, No. 9, 1973, pp. 1328–1330.

[7]Lengelle, G., Kuentzmann, P., and Rendolet, C., "Response of a Solid Propellant to Pressure Oscillations," AIAA and SAE Joint Propulsion Conf., San Diego, CA, Oct. 1974.

[8]De Luca, L., and Galfetti, L., "Combustion Modeling and Stability of Double-Base Solid Rocket Propellants," *Modern Research Topics in Aerospace Propulsion*, edited by G. Angelino, L. De Luca, and W. Sirignano, Springer–Verlag, New York, 1991, pp. 109–134.

[9]Son, S. F., and Brewster, M. Q., "Radiation-Augmented Combustion of Homogeneous Solids," *Combustion Science and Technology*, Vol. 107, 1995, pp. 127–154.

[10]Ibiricu, M. W., and Williams, F. A., "Influence of Externally Applied Thermal Radiation on the Burning Rates of Homogeneous Solid Propellants," *Combustion and Flame*, Vol. 24, 1975, pp. 185–198.

[11]Novozhilov, B. V., *Nonstationary Combustion of Solid Propellants*, Nauka, Moscow (English translation available from National Technical Information Service, AD-767 945), 1973.

[12]Son, S. F., and Brewster, M. Q., "Linear Burning Rate Dynamics of Solids Subjected to Pressure or External Radiant Heat Flux Oscillations," *Journal of Propulsion and Power*, Vol. 9, No. 2, 1993, pp. 222–232.

[13]Novozhilov, B. V., "Stability Criterion for Steady-State Burning of Powders," *Journal of Applied Mechanics and Technical Physics*, No. 4, 1965, pp. 157–160.

[14]Son, S. F., Hites, M. H., and Brewster, M. Q., "An Experimental and Analytical Study of the Unsteady Combustion of Homogeneous Energetic Solids Using the Laser-Recoil Method," Vol. II, Chemical Propulsion Information Agency Publication 593, Oct. 1992, pp. 375–385.

[15]Zebrowski, M. A., "Numerical Modeling of Unsteady Radiation-Driven Combustion of Solids with Condensed Phase Controlled Burning," M.S. Thesis, Univ. of Illinois, Urbana, IL, 1995.

[16]Williams, F. A., *Combustion Theory*, 2nd ed., Addison–Wesley, Reading, MA, 1985, p. 334.

[17]Brewster, M. Q., Zebrowski, M. A., Schroeder, T. B., and Son, S. F., "Unsteady Combustion Modeling of Energetic Solids," AIAA Paper 95-2859, July 1995.

[18]Son, S. F., and Brewster, M. Q., "Unsteady Combustion of Homogeneous Energetic Solids Using the Laser-Recoil Method," *Combustion and Flame*, Vol. 100, 1995, pp. 283–291.

[19]Esker, D. R., and Brewster, M. Q., "Laser Pyrolysis of HTPB," Vol. II, Chemical Propulsion Information Agency Publication 620, Oct. 1994, pp. 235–246; also *Journal of Propulsion and Power*, Vol. 12, No. 2, 1996, pp. 296–301.

[20]Lengelle, G., Bizot, A., Duterque, J., and Trubert, J. F., "Steady-State Burning of Homogeneous Propellants," *Fundamentals of Solid Propellant Combustion*, edited by K. K. Kuo and M. Summerfield, Vol. 90, Progress in Astronautics and Aeronautics, AIAA, New York, 1984, Chap. 7.